Enhancing Practical Multifunctional Myoelectric Applications through Implicit Motor Control Training Systems

Mark Ison and Panagiotis Artemiadis*

Abstract— **Despite holding promise for advances in prostheses and robot teleoperation, myoelectric controlled interfaces have had limited impact in commercial applications. Simultaneous multifunctional controls are desired, but often lead to frustration by users who cannot easily control the devices using state-of-the-art control schemes. This paper proposes and validates the use of implicit motor control training systems (IMCTS) to achieve practical implementations of multifunctional myoelectric applications. Subjects implicitly develop muscle synergies needed to control a robotic application through an analogous visual interface without the associated physical constraints which may hinder learning. The learning then naturally transfers to perceived intuitive and robust control of the robotic device. The efficacy of the method is tested by comparing performance between two groups learning controls implicitly via the visual interface and explicitly via the robotic interface, respectively. The groups achieved comparable performance when performing tasks with the robotic device a week later. Moreover, the initial performance of the experimental group was significantly better than the control group achieved after up to 75 minutes of training. These findings support the use of IMCTS to achieve practical multifunctional control of a wide range of myoelectric applications without limiting them to intuitive mappings nor anthropomorphic devices.**

I. Introduction

Surface electromyography (EMG) has been investigated as a potential input to robotic controls for over half a century. Myoelectric interfaces utilize EMG for real-time, non-invasive access to muscle activity, which is ideal for enhancing many applications in human-machine interaction such as prostheses and robot teleoperation. However, the desire for user-friendly myoelectric applications controlling simultaneous multifunctional robotic devices has yet to be achieved in commercial applications [1], [2].

Simultaneous multifunctional control has often been proposed using pattern recognition techniques, such as artificial neural networks [3] and support vector machines [4], to relate EMG inputs with desired outputs and ultimately predict a user's intent. This approach is limited by the functionality provided in the training set, and restricted by threats of performance degradation during actual use due to transient changes in EMG. Thus, real-time performance requires users to adjust to unpredictable responses for complex motions [5] or restrict controls to those accurately predicted [6].

Other approaches propose fixed mappings with proportional controls, where humans learn to control the application by identifying the relationship between EMG inputs and control outputs. These studies often use EMG signals to control a cursor on a monitor [7]. While interacting with the interface, healthy subjects consistently learn the mapping between input and output, and develop new synergies as they modify muscle activity to correspond with higher-level intent [8]. Learning has been verified in both intuitive (e.g. outputs related to limb motions) and non-intuitive (e.g. random) mapping functions [9]. Pistohl et. al [10] identify similar learning patterns using abstract mappings similar to cursor control to operate a prosthetic hand, and suggest that robotic control can be studied using cursor control paradigms.

This study proposes using visual interfaces beyond studying robotic control, but as implicit motor control training systems (IMCTS) to provide robust and intuitive control of robotic devices. Recent findings by Ison et. al [11] indicate that myoelectric controls learned using a mapping function in one interface transfer to more efficient initial control of other myoelectric interfaces utilizing the same mapping function. This implies that the specific set of muscle synergies developed while interacting with a mapping function are interface independent and can be utilized for efficient control of any robotic device implementing the same mapping function.

IMCTS is validated through a 3 degree of freedom (DOF) robotic arm-hand application with non-intuitive proportional controls. The hand can move along a 2D plane to reach out and grasp objects, with a fixed hand orientation requiring indirect paths to reach an object. An analogous scenario is simulated in a visual interface with 3D pursuit-like tasks, where subjects are instructed to control a helicopter in 3D along specific paths before landing on a target helipad. Subjects learn a common non-intuitive mapping function while interacting with the interface, and increase their control precision by planning movements along the specified paths within time limits. Despite a week between sessions, subjects retain efficiency and then transfer control to intuitive operation of the physical robotic device with performance similar to a control group which only trained with the robot. The implications of this study are vast, as it suggests that IMCTS can be used to train users to operate myoelectric controlled applications without requiring intuitive controls or anthropormorphic devices.

II. Methodology

The experiment is designed to evaluate IMCTS for robust and intuitive control of robotic devices. Six healthy subjects (2 male, 4 female, aged 19-28) are evenly split into two

Mark Ison and Panagiotis Artemiadis are with the School for Engineering of Matter, Transport and Energy, Arizona State University, Tempe, AZ 85287 USA.
Email: {mison, panagiotis.artemiadis}@asu.edu
*Corresponding author.

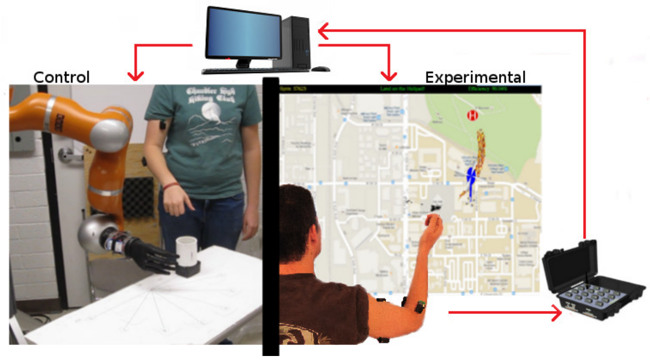

Fig. 1. Experimental setup including the Delsys EMG system and either the robotic or visual interface. The LWR 4 fixes hand orientation and restricts motion to a 2D plane. The subject must control a path around the object before grasping it. Similarly, the visual interface indicates a trajectory for the helicopter before landing on the helipad. The top of the screen indicates an efficiency score based on the percentage of particles collected.

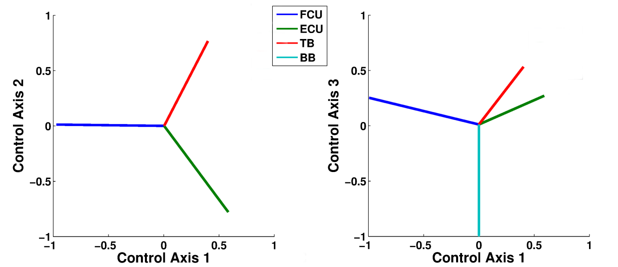

Fig. 2. Mapping of input EMG amplitudes to three output control axes using the mapping function defined in (1).

groups, control and experimental, while learning a non-intuitive control scheme. The control group interacts directly with a 3DOF robotic application using a KUKA Light Weight Robot 4 (LWR 4) and an attached Touch Bionics iLIMB Ultra bionic hand to grasp objects. The experimental group interacts with an analogous 3DOF visual interface to implicitly learn the robot controls. Moving the robot arm in 2D is visually represented as moving a helicopter on the 2D screen, and grasping an object is visually represented as landing the helicopter onto a helipad. Both groups interact with their respective interface over two 50-minute sessions. A testing phase evaluates performance of both groups as they perform a set of tasks with the robotic device. All subjects gave informed consent of the procedures approved by the ASU IRB (Protocol: #1201007252).

A. Experimental Setup

The setup for this experiment is shown in Fig. 1. Four wireless surface EMG electrodes (Delsys Trigno Wireless, Delsys Inc.) are placed on a subject's unconstrained right arm to record muscle activity from the Biceps Brachii (BB), Triceps Brachii (TB), Flexor Carpi Ulnaris (FCU), and Extensor Carpi Ulnaris (ECU). The signals are digitized at 2kHz and sent over TCP/IP as input to a custom program using C++ and OpenGL API [12] to control either interface.

B. Proportional Control

Both interfaces utilize 3 proportional control outputs corresponding to velocities of the 1) 2D planar x-axis, 2) 2D planar y-axis, 3) hand opening/closing and helicopter rising/landing. Raw EMG signals are rectified, filtered (2nd order Butterworth, cut-off 8Hz), and normalized according to each signal's baseline e_b and maximal voluntary contraction e_c, recorded at the start of each experiment: $e = \frac{e_{filt} - e_b}{e_c - e_b}$. The processed signal provides a stable 4×1 input vector $\mathbf{e}$ of normalized EMG amplitudes which is mapped linearly to a 3×1 vector $\mathbf{u}$ of control outputs:

$$\begin{aligned} \mathbf{u} &= g\mathbf{W}\left[(\mathbf{e}-\sigma)\circ u(\mathbf{e}-\sigma)\right], \\ \mathbf{W} &= \begin{bmatrix} -0.9719 & 0.5775 & 0.3944 & 0.000 \\ 0.0118 & -0.7757 & 0.7639 & 0.000 \\ 0.2361 & 0.2544 & 0.5098 & -1.0000 \end{bmatrix} \end{aligned} \quad (1)$$

where $\circ$ is an element-wise matrix multiplicaiton, $u(x)$ is the unit step function, $\sigma = 0.01$ is the muscle activation threshold, and $g = 1.2$ is the output gain. $\mathbf{W}$ is a random matrix optimized with respect to a cost function maximizing the angles between row vectors and subject to the following constraints (see Fig. 2): 1) One column vector is negative along the third control axis, and zero elsewhere, to disconnect grasping/landing from 2D motion. 2) All column vectors are unit length. 3) All row vectors are zero mean to prevent motion at equal co-contractions.

C. Experimental Procedure

The experiment consists of both a learning and testing phase over a three-week span. Subjects are initially shown example tasks with the interface, but not told how EMG maps to control outputs. The learning phase indicates performance trends as each group learns to operate the respective interface. The testing phase compares performance between groups as they both perform tasks with the robotic device.

1) Learning Phase: During the learning phase, subjects interact with either the robot or visual interface for 50 minutes over two separate sessions, with each session separated by one week. Within each session, subjects operate the device for two sets of 25 minutes. Within each set, subjects attempt to perform as many tasks as possible while discovering the control scheme. After each successful task, subjects rest for 7 seconds while the interface resets with a new target. At the end of the learning phase, a subject has interacted with the interface for a total of 100 minutes, 50 minutes each week.

Visual Interface: The visual interface presents a helicopter and a randomly generated path to one of 16 helipads arranged around the unit circle. The helipads are randomly arranged within each cycle of 16 tasks. The path is generated using bezier curves with four control points, with 2000 particles distributed at random offsets along the curve. After an alotted time has passed at a given point on the path, particles turn black and can no longer be collected. A subject's score is reflected by how many particles the helicopter collects on the way to the helipad. A perfect score can be achieved by traversing the center of the path within eight seconds,

Fig. 3. Hand configuration in testing phase. Left: normal configuration from learning phase. Right: rotated configuration.

encouraging constant improvements in both speed and precision while learning controls. Each task is complete once the helicopter lands on the helipad.

Robot Interface: The robot interface presents the iLIMB hand which can move along a 2D plane to grasp a cylindrical object at one of 8 different locations arranged around a semicircle. The locations are randomly arranged to appear twice within each cycle of 16 tasks, and, due to the fixed hand orientation, subjects must move the hand along a specific path in order to approach and grasp the object. If the object is knocked off its location, the experimenter places it back. Each task is complete once the hand grasps the object.

2) Testing Phase: The testing phase occurs a week after completion of the learning phase. Both groups control the robot interface, performing the same tasks as in the learning phase for the control group, with an additional objective of returning the object to the starting position. Moreover, after 2 cycles, or 32 tasks, the hand is rotated, as shown in Fig. 3. The changes are made to evaluate performance over generalized tasks within the same control space. The experimental group is informed that the controls require similar commands as learned in the visual interface, but are not given the exact relationship, and the control group is assured the controls are the same as the previous two weeks.

D. Data Analysis

Performance is measured in the visual interface by completion time and path efficiency. Completion time is defined as the time elapsed from the start of the task until the helicopter lands on the helipad. Path efficiency is represented by the percentage of total particles collected for each trial measuring both speed and precision as a robust metric for overall control efficiency. Performance is measured for the robotic interface by completion time, defined as the time elapsed from the start of the task to grasping the object.

III. Results

IMCTS is evaluated with respect to performance trends from each group in the learning phase and direct performance comparisons between the groups in the testing phase.

A. Learning Phase

Due to the non-intuitive control scheme, each subject experiences a large learning curve with variable learning rates according to how efficiently the subject explores the control space. Although both interfaces are similar in terms of required inputs to complete a task, the visual interface is capable of consistently better completion times due to the lack of physical constraints such as joint velocity limits with

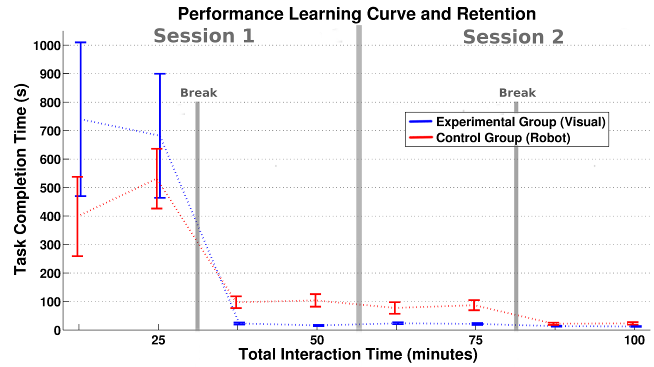

Fig. 4. Completion time as a function of total training time for all subjects in the learning phase. The errorbars represent a 95% confidence interval for aggregated completion times over each half of each set. The consistent improvement, despite a week between sessions, indicates the subjects are achieving robust control.

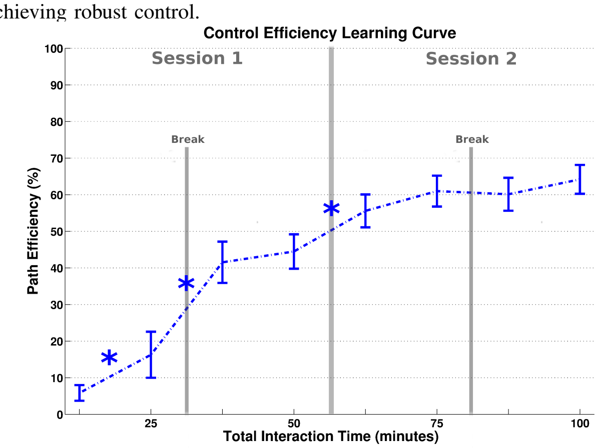

Fig. 5. Control efficiency as a function of total training time for all subjects in the learning phase experimental group. The errorbars represent a 95% confidence interval for aggregated task efficiencies over each half of each set. Asterisks indicate significant improvements between adjacent points (Welch's t-test, $p < 0.05$).

the LWR 4, variable delays in Bluetooth communication with the iLIMB, and replacing the object if it is knocked off its location. These physical constraints slow the learning rate of the control group, as visual feedback sometimes reinforces incorrect mappings between input and outputs.

Figure 4 displays the learning curves of both groups with average completion times as a function of total training time. Each 25 minute set of trials produces two data points, the first representing completion times over the first 12.5 minutes, and the second representing aggregated completion times over the second half of the set. The experimental group generally improved performance within each set as they refined controls. In constrast, the control group generally lowered performance between the two halves of each set. Qualitative feedback from subjects suggests this results from tension and fatigue due to inconsistent visual feedback. This effect is reduced as subjects learn better control over time.

Despite having a week between sessions, both groups demonstrate performance robust to significant degradation, with the control group achieving significantly better performance between the end of session 1 and the start of session 2 (Welch's t-test, $p < 0.05$). The experimental group traded slower performance in exchange for significantly better effi-

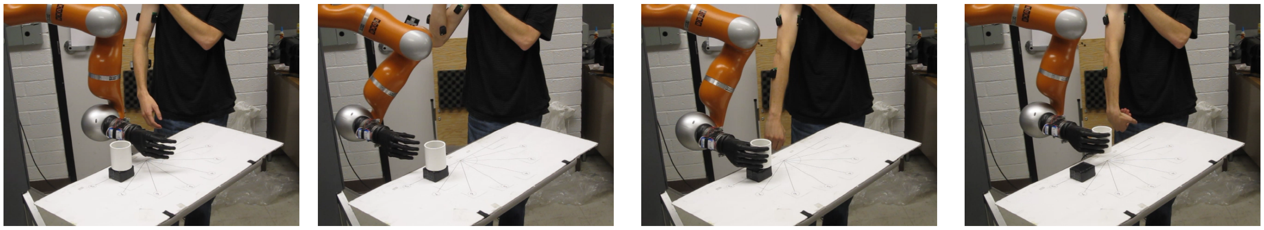

(a) Beginning of trial. (b) Moving around the object. (c) Grasping the object. (d) Returning object to start point.

Fig. 6. Trial sequence for robot control tasks. With the hand in a fixed orientation, the subject moves around the object before grasping and retrieving it.

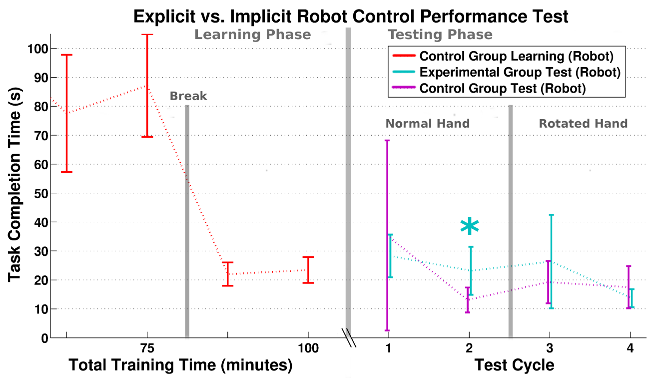

Fig. 7. Comparison of completion times between groups relative to the performance of the control group in the second session of the learning phase. The errorbars represent a 95% confidence interval for aggregated completion times over each cycle of 16 tasks. The asterisk above cycle 2 indicates the only significant performance difference between the two groups (Welch's t-test, $p < 0.5$).

ciency (Welch's t-test, $p < 0.05$), as shown in Fig. 5. At the conclusion of the 100 minute learning phase, subjects had generally learned the mappings associating muscle activity with control outputs, but had not yet achieved consistent performance associated with fully developed muscle synergies.

B. Testing Phase

Completion times from the testing phase validate the use of IMCTS for robust robotic control. An example task sequence is shown in Fig. 6. Despite a week off and not knowing how controlling the helicopter relates to controlling the robotic hand, subjects in the experimental group are able to transfer their learning to intuitively perform the tasks comparable to the control group, with initial performance significantly better than the control group achieved after 75 minutes of total training time (Welch's t-test, $p < 0.05$, see Fig. 7). In addition, both groups adjust to tasks with the rotated hand without a significant reduction in performance (Welch's t-test, Experimental: $p = 0.73$, Control: $p = 0.15$), indicating robust control of the full task space. During the fourth cycle in the test phase, the experimental group performed slightly better than the control group (Welch's t-test, $p = 0.17$), and significantly better than the control group after 100 minutes of trianing (Welch's t-test, $p < 0.05$). This, combined with the consistent learning shown in Figs. 4 and 5, supports IMCTS as a viable tool in robotic control.

IV. Conclusion

This paper validates the use of implicit motor control training systems to achieve intuitive and robust control of myoelectric applications. Subjects implicitly develop motor control patterns needed to control a physical robotic application through an analogous visual interface without the associated physical constraints which may hinder learning. During the learning process, subjects consistently enhance performance even after time off, corresponding to robust identification of the non-intuitive mapping function. Despite having a week off between sessions, subjects intuitively transferred their learning to efficiently control the robotic device, with performance similar to the control group which had learned the controls by explicitly operating the robotic device for the same amount of time. These findings support the use of IMCTS to achieve practical multifunctional control of a wide range of myoelectric applications without limiting them to intuitive mappings nor anthropomorphic devices.

References

[1] A. Simon, L. Hargrove, B. Lock, and T. Kuiken, "A Decision-Based Velocity Ramp for Minimizing the Effect of Misclassifications During Real-Time Pattern Recognition Control," *Biomedical Engineering, IEEE Transactions on*, vol. 58, no. 8, pp. 2360–2368, 2011.

[2] E. Scheme and K. Englehart, "Electromyogram pattern recognition for control of powered upper-limb prostheses: state of the art and challenges for clinical use." *Journal of rehabilitation research and development*, vol. 48, no. 6, pp. 643–659, 2010.

[3] M. R. Ison and P. Artemiadis, "Beyond User-Specificity for EMG Decoding Using Multiresolution Muscle Synergy Analysis," in *Dynamic Systems and Control Conference, 2013 (DSCC 2013)*. ASME, 2013.

[4] G. Naik, D. Kumar, and Jayadeva, "Twin SVM for Gesture Classification Using the Surface Electromyogram," *Information Technology in Biomedicine, IEEE Transactions on*, vol. 14, no. 2, pp. 301–308, Mar 2010.

[5] N. Jiang, I. Vujaklija, H. Rehbaum, B. Graimann, and D. Farina, "Is accurate mapping of emg signals on kinematics needed for precise online myoelectric control?" *Neural Systems and Rehabilitation Engineering, IEEE Transactions on*, vol. PP, no. 99, pp. 1–1, 2013.

[6] A. E. Gibson, M. R. Ison, and P. Artemiadis, "User-Independent Hand Motion Classification with Electromyography," in *Dynamic Systems and Control Conference, 2013 (DSCC 2013)*. ASME, 2013.

[7] S. M. Radhakrishnan, S. N. Baker, and A. Jackson, "Learning a novel myoelectric-controlled interface task," *J Neurophysiol*, vol. 1, p. 47, 2008.

[8] K. Nazarpour, A. Barnard, and A. Jackson, "Flexible Cortical Control of Task-Specific Muscle Synergies," *Journal of Neuroscience*, vol. 32, no. 36, pp. 12 349–12 360, Sep 2012.

[9] C. W. Antuvan, M. Ison, and P. Artemiadis, "Embedded human control of robots using myoelectric interfaces," *Neural Systems and Rehabilitation Engineering, IEEE Transactions on*, vol. PP, no. 99, pp. 1–1, 2014.

[10] T. Pistohl, C. Cipriani, A. Jackson, and K. Nazarpour, "Adapting proportional myoelectric-controlled interfaces for prosthetic hands," in *Engineering in Medicine and Biology Society (EMBC), 2013 35th Annual International Conference of the IEEE*, July 2013, pp. 6195–6198.

[11] M. Ison, C. W. Antuvan, and P. Artemiadis, "Learning Efficient Control of Robots Using Myoelectric Interfaces," in *Robotics and Automation, 2014 (ICRA 2014), IEEE International Conference on*, 2014 (to appear).

[12] [Online]. Available: http://www.opengl.org